ISSN 2072-5981
doi: 10.26907/mrsej

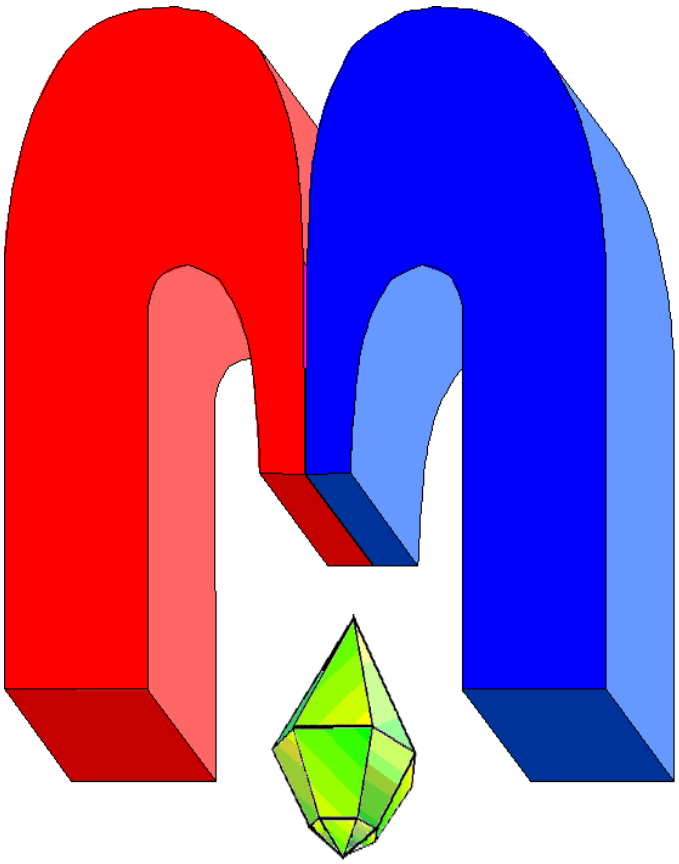

Magnetic Resonance in Solids

Electronic Journal

Volume ***21***
Special Issue ***3***
Paper No ***19310***
1-13 pages
2019
doi: **10.26907/mrsej-19310**

http://mrsej.kpfu.ru
http://mrsej.ksu.ru

Established and published by Kazan University
Endorsed by International Society of Magnetic Resonance (ISMAR)
Registered by Russian Federation Committee on Press (#015140), August 2, 1996
First Issue appeared on July 25, 1997

"***Magnetic Resonance in Solids. Electronic Journal***" (**MRS*ej***) is a peer-reviewed, all electronic journal, publishing articles which meet the highest standards of scientific quality in the field of basic research of a magnetic resonance in solids and related phenomena.

Indexed and abstracted by
Web of Science (*ESCI*, Clarivate Analytics, from 2015), *Scopus* (Elsevier, from 2012), *RusIndexSC* (*eLibrary*, from 2006), *Google Scholar*, *DOAJ*, *ROAD*, *CyberLeninka* (from 2006), *SCImago Journal & Country Rank*, etc.

* In Kazan University the Electron Paramagnetic Resonance (EPR) was discovered by Zavoisky E.K. in 1944.

Short cite this: *Magn. Reson. Solids* **21**, 19310 (2019) doi: 10.26907/mrsej-19310

Resonant magnetoresistance in double-barrier antiferromagnetic tunnel junction

N.Kh. Useinov

Institute of Physics, Kazan Federal University, Kremlevskaya 18, Kazan 420008, Russia

E-mail: Niazbeck.Useinov@kpfu.ru

(Received March 23, 2019; accepted March 31, 2019; published April 19, 2019)

Resonant tunneling is studied theoretically for the asymmetric double-barrier antiferromagnetic tunnel junction (DAMTJ) with a bias voltage is applied. In this nanostructure, the direction of magnetization of the middle ferromagnetic layer is parallel (antiparallel) to the direction of magnetization of the top layer and antiparallel (parallel) to the direction of magnetization of the bottom ferromagnetic layer. Analytical expression for the transmission coefficient of the double-barrier nanostructure is received, which is expressed through single-barrier transmission coefficients taking into account the voltage drop on each barrier and spin degrees of freedom of the electron conductivity. The theoretical model of spin-polarized conductance and tunnel magnetoresistance in asymmetric DAMTJ in the quasi-classical approximation is developed. The dependences of the transmission coefficient and tunnel magnetoresistance on the applied voltage under resonant conditions are shown.

PACS: 72.25.-b, 73.40.Gk, 75.76.+j, 75.75.-c.

Keywords: spin-polarized conductance, magnetic tunnel junction, nanostructures, tunnel magnetoresistance.

This work, dedicated to the 85th anniversary of my teacher, Professor B.I. Kochelaev, represents the latest research carried out by the author in recent years

1. Introduction

High tunneling magnetoresistance (TMR) is now well known in Fe/MgO/Fe and CoFe(B)/MgO/CoFe(B) magnetic tunnel junctions (MTJs). Besides single barrier MTJs (SBMTJs), double barrier MTJs (DBMTJs) have also extensively studied and investigate for the novel physical properties and applications in spintronics devices [1, 2]. Compared with SBMTJs, DBMTJs have larger $V_{1/2}$ (voltage where TMR decreases to its half maximum value), which is desirable for practical applications. With a thin ferromagnetic (FM) layer sandwiched by two MgO layers, quantum well states can lead to oscillations in the transmission as a function of interlayer thickness [3], also Coulomb blockade and Kondo-assisted tunneling phenomena have been reported [4]. Besides these phenomena, quantum well state and resonant tunneling could also be observed in double-barrier tunnel junction [5,6]. It is well known that the resonance condition for the symmetrical double-barrier structure is a basis for understanding the resonance phenomena in symmetrical multibarrier structures.

For the first time theoretical study of resonant tunneling has been made by Breit and Wigner, in the context of resonant enhancement of the neutron capture cross section observed in nuclear physics [7]. Resonant tunneling has since become relevant for solid state physics as well, in particular because of the proposal by Tsu and Esaki [8] to build multiple barrier "superlattice" devices using semiconductor heterostructures. Evidence for resonant tunneling through a double barrier structure was first reported by Chang, Esaki and Tsu [9]. As in most of the subsequent experiments, they measured the current-voltage characteristic to detect the resonance as a negative differential resistance at finite bias. Although a lot of studies have been made, the tunneling mechanisms in both SBMTJs and DBMTJs are still unclear. Generally, the value of the trans-

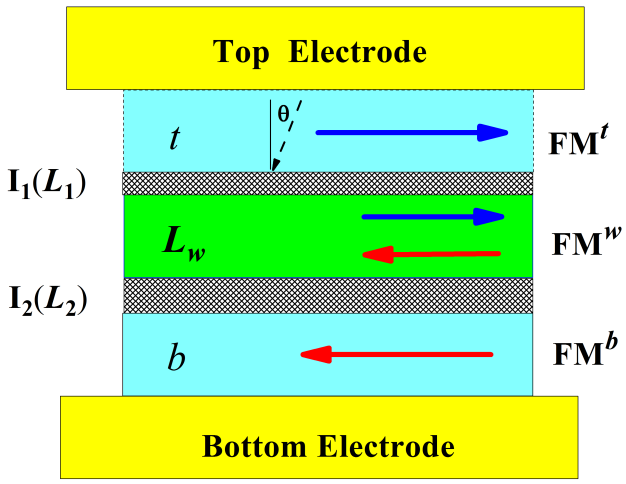

Figure 1. Schematic drawing of the cross section of the asymmetrical double-barrier antiferromagnetic tunnel junction is shown. The top t and bottom b of ferromagnetic layers are electrodes of the junction, L_w is the thickness of the middle ferromagnetic layer; L_1 and L_2 are the thickness of the insulators. Arrows indicate the magnetization of the electrodes and the middle ferromagnetic layer in the parallel and antiparallel alignments. The small dashed arrow indicates the direction of the electron conduction trajectory with the incidence angle θ_t measured from the z-axis, which perpendicular to the layers.

mission coefficient of conduction electron is reduced when a voltage is applied. Therefore, it is very important for device designing to investigate the resonance conditions by taking into account the effect of electric field. Several theoretical studies for resonant tunneling phenomena in double-barrier quantum well structures under an applied voltage have been performed by using the multistep rectangular approximation, real-time diagrammatic technique [10] or the Airy function with quasi-classical approximation [11, 12].

In this article we derive an analytical expression of the transmission coefficient and the resonance conditions in an asymmetric double-barrier antiferromagnetic tunnel junction (DAMTJ). We demonstrate the existence of sharp spin-dependent quantum well states within the middle FM layer from calculation of the transmission coefficient and round-trip phase shift at an applied voltage. The dependences of the TMR on the applied voltage under resonant conditions are shown, see Sec. 4. In DAMTJ, the direction of magnetization of the top FM layer is antiparallel to the alignment of magnetization of the bottom FM layer; while the middle FM layer can change its direction of magnetization, see Fig. 1. The resonant tunneling transmission characteristics are studied theoretically in more detail by taking into account mass difference between the FM layers and the barrier layers. In this structure, we can obtain a comparatively low resonance spin-depended level which may be favorable for device applications. In Sec. 3, the analytical expressions for the transmission coefficient and the resonance condition are derived by using the Airy function and transfer matrix method. In Sec. 4, the spin-polarized conductance through the DAMTJ is calculated on the basis of the quasi-classical theory [13]. The basic mathematical expressions and calculation details can be found in article [14]. The final section is a summary.

2. Model of asymmetrical DAMTJ

As shown in Fig. 1, the DAMTJ consist of three planar ferromagnetic layers of thicknesses t, L_w and b, respectively, separated by two a nonmagnetic insulators of thicknesses L_1 and L_2 of several angstroms. This gives a three-dimensional model of the double-barrier antiferromagnetic nanostructure $\mathrm{FM}^t/\mathrm{I}_1/\mathrm{FM}^w/\mathrm{I}_2/\mathrm{FM}^b$, because the magnetization of the layers FM^t and FM^b is

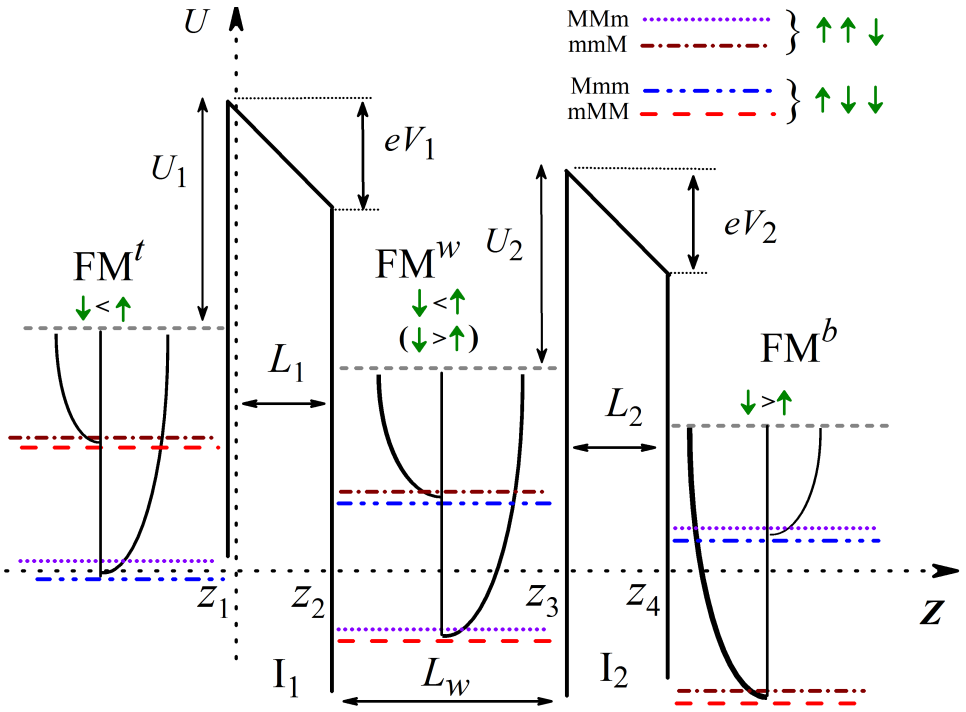

Figure 2. Schematic planar potential barriers separating three degenerate electron gas regions of equal chemical potential, but with shifted Fermi levels because of the voltage V applied across the barriers are shown. The dispersion laws of the spin sub-bands of majority (M) of the electrons and the spin sub-bands of minority (m) of the electrons in FM layers with antiferromagnetic alignment of magnetizations also are shown. The notation $\downarrow<\uparrow$ for the FM^t layer means that the magnetization of the layer is aligned upward. The arrows inside the brackets ($\downarrow>\uparrow$) correspond to the case when the magnetization in the FM^w layer is inverted. Then, the direction of magnetization in the FM^w layer will correspond to the magnetization direction (downward) of the FM^b layer. The electron spin-conduction channels passing through the minority (m) and/or majority (M) spin sub-bands are shown by lines: short-dot, dash-dot, dash-dot-dot and dashed. The U_1 and U_2 are the heights of the barriers above Fermi energy. The V_1 and V_2 are voltage drop across the first and second barriers, respectively.

always directed antiparallel. Typical materials for the constituents of the junction are Co, CoCr, CoFeB, Fe, and NiFe for ferromagnets and Al_2O_3 and MgO for insulating nonmagnetic barriers. Note, that FM^w layer is with a lower coercivity as compared to the FM^t and FM^b layers.

The one-dimensional schematic energy diagram of the asymmetrical double-barrier structures under an applied voltage is shown in Fig. 2, where L_1 and U_1 are the barrier width and the barrier height for the left-hand side barrier layer, L_2 and U_2 are those for the right-hand one, L_w, is the well width. The five regions are specified by the coordinates z_1, z_2, z_3 z_4. The double planar barrier is forming a quantum well with quasi-bound state at energy E_R. The voltage drop in the left-hand side barrier (top insulating layer I_1) and that in the right-hand (bottom insulating layer I_2) one are by the following equations:

$$V_1 = \frac{\varepsilon_2 L_1}{\varepsilon_1 L_2 + \varepsilon_2 L_1} V, \qquad V_2 = \frac{\varepsilon_1 L_2}{\varepsilon_1 L_2 + \varepsilon_2 L_1} V, \tag{1}$$

where V is the total applied voltage, $\varepsilon_{1,2}$ are the dielectric permittivities of the barriers.

In the Fig. 2 the large parabolas represent dispersion law for the electrons from the majority (M) conductance spin sub-bands. The small parabolic curves belong to electrons of the minority (m) conductance spin sub-bands. The arrows above the Fermi level show the direction magneti-

zations of the FM layers. The notation $\downarrow<\uparrow$ for the FM^t layer means that the magnetization of the layer is aligned upward. The arrows inside the brackets ($\downarrow>\uparrow$) correspond to the case when the magnetization in the FM^w layer is inverted. Then, the direction of magnetization in the FM^w layer will correspond to the magnetization direction of the FM^b layer. The electron spin-conduction channels passing through the minority and/or majority spin sub-bands are shown by lines: dash-dot-dot, dashed, short-dot and dash-dot. The Fermi energy E_F origin is taken at the bottom of the conduction band of the region FM^w material.

Consider the ballistic motion of an electron through DAMTJ assuming that the electron with energy E_F is incident from the left (in Fig. 1 with top) and transmits to the right along the axis z direction (in Fig. 1, downward). For the antiferromagnetic alignment of the magnetizations of the top and bottom $FM^{t(b)}$ electrodes the middle layer FM^w may invert direction of the magnetizations, then the electron with spin up, $s=\uparrow$, moves in the following spin sub-bands: MMm and Mmm. These are two spin channels of conduction. For the electron with spin down $s=\downarrow$ alignment the electron moves in the following spin sub-bands: mMM and mmM. These are another two spin channels of conduction. Note that in our model the direction of the conduction electron spin $s=\uparrow(\downarrow)$ is conserved during the tunnel and resonance. Here, we assume that the effect of the space charge built up in the quantum well is neglected, that the voltage drop occurs only across the barrier regions. The conduction band edge is flat with zero field for simplicity in the three FM regions (FM^t, FM^w and FM^b).

3. Transmission coefficient and resonance condition

In the section, we will derive analytical expressions for the transmission coefficient and the resonance condition in asymmetrical double-barrier structures with quantum well under a dc bias field. For these it is necessary to find the full wave function $\Psi_s(z;k_x,k_y)$, where k_x,k_y are the components of the wavevector that satisfy the law of momentum conservation under a dc bias field. In the one-dimensional case, the states of motion of the conduction electron can be found from solutions of the Schrodinger equation. The solutions of the Schrödinger equations for the electron in all FM regions and that in the trapezoidal potential regions (barrier regions) are well known (see for example [15]). Another equivalent description is via the transfer matrix [11, 16]. The transfer matrices are equivalent descriptions for transmission through the intermediate region of the heterostructures. A convenient property of the transfer matrix is the multiplicative composition rule: the transfer matrix of a number of disordered regions in series separated by ideal leads is the product of the individual transfer matrices. To be more explicit consider the local, single-particle potential $U(z)$ in the Hamiltonian of the system. The potential is piecewise smooth and it is assumed that the fundamental set of solutions of the Schrödinger equation in the FM subspaces $\left\{\varphi^+_{l,s}(z),\varphi^-_{l,s}(z)\right\}$, $l\in\{t,w,b\}$ are known. The fundamental set of solutions of the Schrödinger equation in the appropriate insulators are $\left\{\psi^+_{l,s}(z),\psi^-_{l,s}(z)\right\}$, $l\in\{1,2\}$. Therefore, the transfer matrix for transporting the wave function consists of a linear combination of eigenfunctions with appropriate coefficients $A_{l,s}$, $B_{l,s}$, and their derivatives in the interval $[t,b]$. A free wave $\varphi^+_{t,s}(z)=\sqrt{m_t/k_{t,s}}\exp\left(ik_{t,s}z\right)$ incident from the top is scattered off the potentials and partly transmitted to the bottom, $\varphi^+_{b,s}(z)=\sqrt{m_b/k_{b,s}}\exp\left(ik_{b,s}z\right)$, where $k_{t(b),s}$ are the components of Fermi wavenumbers for electrons of spin sub-bands of $FM^{t(b)}$ layers and $m_{t(b)}$ are the effective masses. The wave function in FM^w layer have the same form $\varphi^+_{w,s}(z)=\sqrt{m_w/k_{w,s}}\exp\left(ik_{w,s}z\right)$. Matching of these functions leads to the following equation for the transfer matrix:

$$\begin{pmatrix} A_{b,s} \\ B_{b,s} \end{pmatrix} = \mathbf{TM}_{2b,s} \begin{pmatrix} A_{t,s} \\ B_{t,s} \end{pmatrix}, \tag{2}$$

where we identify $A_{t,s} = a_{\text{in}}$, $B_{t,s} = b_{\text{out}}$, $A_{b,s} = a_{\text{out}}$, $B_{b,s} = b_{\text{in}}$ in terms of in- and out-scattering states of the conductor. For example, the transfer matrix for the first barrier is determined by the product of matrices

$$\begin{aligned} \mathbf{TM}_1 = & \begin{pmatrix} \varphi_w^+(z_2) & \varphi_w^-(z_2) \\ \varphi'^+_w(z_2) & \varphi'^-_w(z_2) \end{pmatrix}^{-1} \begin{pmatrix} \psi_1^+(z_2) & \psi_1^-(z_2) \\ \psi'^+_1(z_2) & \psi'^-_1(z_2) \end{pmatrix} \times \\ & \times \begin{pmatrix} \psi_1^+(z_1) & \psi_1^-(z_1) \\ \psi'^+_1(z_1) & \psi'^-_1(z_1) \end{pmatrix}^{-1} \begin{pmatrix} \varphi_t^+(z_1) & \varphi_t^-(z_1) \\ \varphi'^+_t(z_1) & \varphi'^-_t(z_1) \end{pmatrix}. \end{aligned} \tag{3}$$

Here and further for simplicity we omit the spin index. Similarly, you can find the transfer matrix $\mathbf{TM}_2$ for the second barrier. The conservation of probability density in stationary state implies that $\det \mathbf{TM}_{1(2)} = 1$. Transfer matrix the whole system can be found from the product of matrices $\mathbf{TM}_1$ and $\mathbf{TM}_2$: $\mathbf{TM}_{2b} = \mathbf{TM}_2 \cdot \mathbf{TM}_1$. From the transmission matrix $\mathbf{TM}_{2b}$ the transmission coefficient through the system can be calculated.

After using a straightforward algebra, can derive the total transmission coefficient $T_{2b}^{\text{P(AP)}}$ with an applied voltage and taking into account of spin degree of freedom:

$$\begin{aligned} T_{2b}^{\text{P(AP)}} = \frac{|a_{\text{out}}|^2}{|a_{\text{in}}|^2} = \Big[& T_1^{-1} T_2^{-1} + \left(T_1^{-1} - 1\right)\left(T_2^{-1} - 1\right) + \\ & + 2\sqrt{T_1^{-1}\left(T_1^{-1} - 1\right)}\sqrt{T_2^{-1}\left(T_2^{-1} - 1\right)}\cos\Phi_V \Big]^{-1}, \end{aligned} \tag{4}$$

where we have

$$T_1 = \frac{4m_1 m_t m_w k_t k_w t_1^2/\pi^2}{\left(\beta_1 - \gamma_1\right)^2 + \left(\chi_1 + \alpha_1\right)^2}, \qquad T_2 = \frac{4m_2 m_w m_b k_w k_b t_2^2/\pi^2}{\left(\beta_2 - \gamma_2\right)^2 + \left(\chi_2 + \alpha_2\right)^2}, \tag{5}$$

of the transmission coefficients in the top side single barrier and the bottom one and $\Phi_V = \phi_1 + \phi_2 + 2k_w L_w$ is the total phase shift for one round-trip in the quantum well. Here ϕ_1 and ϕ_2 are the phase shifts incurred on reflection off the barriers during propagation of an electron wave. These phases are defined by the formulas

$$\phi_1 = \arctan\left[\frac{2\left(\chi_1\gamma_1 + \beta_1\alpha_1\right)}{\chi_1^2 - \gamma_1^2 + \beta_1^2 - \alpha_1^2}\right], \qquad \phi_2 = \arctan\left[\frac{2\left(\chi_2\beta_2 + \gamma_2\alpha_2\right)}{\beta_2^2 - \chi_2^2 - \gamma_2^2 + \alpha_2^2}\right]. \tag{6}$$

In the Eqs. (5) and (6) the following notation of linear combinations of Airy functions are used:

$$\begin{aligned} \alpha_l &= m_l^2 k_{t(w)} k_{w(b)} \left\{\text{Ai}\left[q_l(0)\right]\text{Bi}\left[q_l(L_l)\right] - \text{Bi}\left[q_l(0)\right]\text{Ai}\left[q_l(L_l)\right]\right\}, \\ \beta_l &= m_l m_{w(b)} k_{t(w)} t_l \left\{\text{Ai}\left[q_l(0)\right]\text{Bi}'\left[q_l(L_l)\right] - \text{Bi}\left[q_l(0)\right]\text{Ai}'\left[q_l(L_l)\right]\right\}, \\ \gamma_l &= m_l m_{t(w)} k_{w(b)} t_l \left\{\text{Ai}'\left[q_l(0)\right]\text{Bi}\left[q_l(L_l)\right] - \text{Bi}'\left[q_l(0)\right]\text{Ai}\left[q_l(L_l)\right]\right\}, \\ \chi_l &= m_{t(w)} m_{w(b)} t_l^2 \left\{\text{Ai}'\left[q_l(0)\right]\text{Bi}'\left[q_l(L_l)\right] - \text{Bi}'\left[q_l(0)\right]\text{Ai}'\left[q_l(L_l)\right]\right\}, \end{aligned} \tag{7}$$

where $\text{Ai}'\left[q_l\right]$ and $\text{Bi}'\left[q_l\right]$ are the first derivatives of the Airy functions, t_l is the factor (see also Eqs. (5)) has the form $t_l = \left(2m_l eV_l/\hbar^2 L_l\right)^{1/3}$, for the subscript $l = 1, 2$. The arguments $q_l(z)$ of the Airy functions for our problem can be written as

$$q_l(z) = t_l \left(z + \frac{\hbar^2 L_l \left(k_{\text{F}}^{t(w)}\right)^2}{2m_l eV_l} - \frac{L_l\left(E_{\text{F}} + U_l\right)}{eV_l} \right). \tag{8}$$

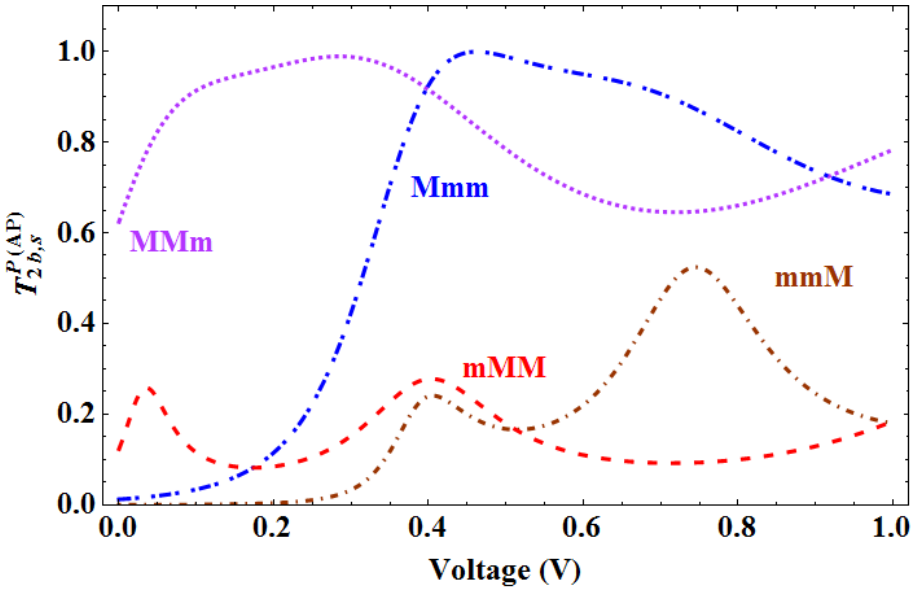

Figure 3. Dependences of the total transmission coefficient vs applied bias across the asymmetrical DAMTJ for four spin conduction channels designated in accordance with Fig. 2.

The results of the calculation of the transmission coefficients (4) with the parameters corresponding to the experimental data are shown in Fig. 3. These dependences are of the total transmission coefficient on the applied voltage V for four spin channels MMm, mmM, Mmm and mMM of conductivity. The curves were calculated with the following parameters of the structure. The values of the Fermi wavevectors for electrons of spin sub-bands of FM layers were taken: $k^t_{\mathrm{F},\uparrow} = 1.1\,\text{Å}^{-1}$, $k^t_{\mathrm{F},\downarrow} = 0.98\,\text{Å}^{-1}$, $k^b_{\mathrm{F},\uparrow} = 1.04\,\text{Å}^{-1}$, $k^b_{\mathrm{F},\downarrow} = 0.975\,\text{Å}^{-1}$, and $k^w_{\mathrm{F},\uparrow} = 1.0\,\text{Å}^{-1}$, $k^w_{\mathrm{F},\downarrow} = 0.97\,\text{Å}^{-1}$, respectively.

The effective masses of conduction electrons in the ferromagnetic layers corresponded to the free electron mass m_e. Two dielectric oxide layers had transverse sizes comparable to the mean free path of conduction electrons. There have thicknesses $L_1 = 15.0\,\text{Å}^{-1}$, $L_2 = 19.0\,\text{Å}^{-1}$ and heights of the energy potentials above of Fermi energy are $U_1 = 0.24\,\text{eV}$, $U_2 = 0.18\,\text{eV}$. The dielectric constant in the first barrier is $\varepsilon_1 = 10.1$ and that in second barrier $\varepsilon_2 = 9.8$, see Ref. [17]. The effective masses of the electrons in the barriers were assumed to be $m_{1(2)} = 0.4m_e$ [18]. The thickness of the medial FM^w layer equalled $L_w = 25.0\,\text{Å}$.

Next, let us investigate the resonance condition in the model studied here. Because of $0 < T_{1,s} < 1$ and $0 < T_{2,s} < 1$, as seen in Eq. (4), it is understood that $T^{\mathrm{P(AP)}}_{2b,s}$ shows a local minimum for $\cos\Phi_{V,s} = 1$ and a local maximum for $\cos\Phi_{V,s} = -1$. Then for

$$\Phi_{V,s} = \pi + \phi_{1,s} + \phi_{2,s} + 2k_{w,s}L_w = \pi(2n+1), \qquad (n = 0,\ 1,\ 2, ...) \tag{9}$$

we obtain the local maximum value of the transmission coefficient by

$$T^{\mathrm{P(AP)}}_{2b,\mathrm{max},s} = \left[\sqrt{T^{-1}_{1,s}T^{-1}_{2,s}} - \sqrt{\left(T^{-1}_{1,s} - 1\right)}\sqrt{\left(T^{-1}_{2,s} - 1\right)}\right]^{-2}. \tag{10}$$

The phase difference (9) with $n = 8$ for each spin conduction channel in the asymmetrical DAMTJ gives the values of the resonance voltages, see Fig. 4. At these voltages, the transmission coefficient $T^{\mathrm{P(AP)}}_{2b,s}$ for each spin conduction channel takes the maximum value, see Fig. 3.

The energy dependent transmission coefficient $T^{\mathrm{P(AP)}}_{2b,s}(E)$ may be obtained from Eq. (4) provided the phase shift $\Phi_{V,s}$ and the transmission coefficients of the individual barriers (5) are

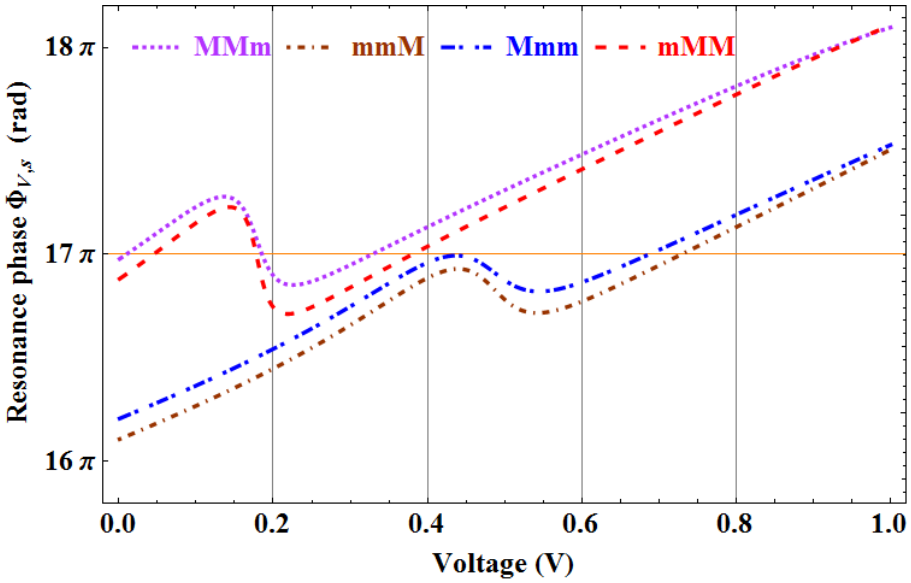

Figure 4. The resonance phase as a function of the applied voltage calculated with the same parameters as in Fig. 3. The four curves correspond to the spin conduction channels of electron.

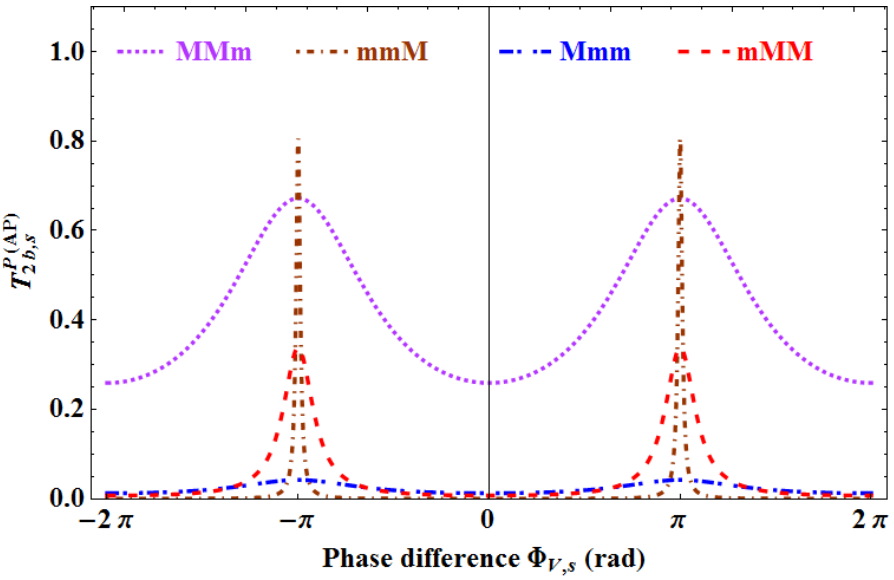

Figure 5. The transmission coefficients as a function of the phase difference $\Phi_{V,s}$ under applied voltage of $V = 0.01$ V are shown. The curves are calculated with the same parameters as in Fig. 3. The four curves correspond to the spin conduction channels of electron.

known as a function of energy. The transmission coefficients $T_{2b,s}^{\mathrm{P(AP)}}(E)$ has a maximum whenever $\Phi_{V,s} = \pi(2n+1)$, as a consequence of destructive interference of the backscattered partial waves. Since this is precisely the condition for the existence of a quasi-bound state in the quantum well, the resonance occurs when the energy of the incident electron coincides with the energy E_{R} of a quasi-bound state. If $T_{1,s} = T_{2,s} = T_s$ and (9) are satisfied, then resonance conditions occur, which lead to the maximum peak value of the transmission coefficient $T_{2b,s}^{\mathrm{P(AP)}}(E)$. Note that if the double barrier structure is symmetric ($T_{1,s} = T_{2,s} = T_s$), the maximum transmission coefficient is unity, regardless of the magnitude of the barrier transparencies.

The transmission coefficients through the DAMTJ as a function of the round-trip phase shift $\Phi_{V,s}$, calculated from Eqs. (4) and (6) are shown in Fig. 5. The plots of $T_{2b,s}^{\mathrm{P(AP)}}$ as a function of

$\Phi_{V,s}$ were computed under applied voltage of $V = 0.01$ V for the same parameters as in Fig. 3. If the barriers are sufficiently high and thick, both $T_{1,s} \ll 1$ and $T_{2,s} \ll 1$, and $T_{2b,s}^{\mathrm{P(AP)}}(E)$ reduces to the Breit-Wigner form for energies close to a resonance [19] and plots $T_{2b,s}^{\mathrm{P(AP)}}(E)$ will be similar of Fig. 5. Next we will discuss it.

The phase shifts incurred on reflection off the barriers are $\phi_{l,s} = -\pi/2$, independent of energy, see Eq. (9). If the separation of the barriers is L_w, then the resonance condition $\Phi_{V,s} = \pi(2n+1)$ reduces to the familiar Bohr-Sommerfeld quantization condition $2L_w/\lambda = n + 1/2$ (here $\lambda = 2\pi/k$, with $k = \sqrt{2mE}/\hbar$). Consider one such state, at resonance energy E_{R}. For energies close to E_{R} the round-trip phase shift $\Phi_{V,s}$ is linear in $\varepsilon_{\mathrm{R}} \equiv E - E_{\mathrm{R}}$, therefore we have

$$\frac{d\Phi_{V,s}}{dE} = \frac{d\Phi_{V,s}}{dk_{w,s}}\frac{dk_{w,s}}{dE} = 2L_w\left(\frac{\pi\rho_s}{L_w}\right) = \frac{1}{\hbar\nu_s}, \tag{11}$$

where $\nu_s = 1/2\pi\hbar\rho_s$ is the attempt frequency and $\rho_s = (L_w/\pi)\, dk_{w,s}/dE$ is the density of states in the quantum well. Close to resonance we may thus write

$$\Phi_{V,s} \approx \pi(2n+1) + \varepsilon_{\mathrm{R}}/\hbar\nu_s\,. \tag{12}$$

By expanding $\cos\Phi_{V,s} \approx 1 - (\varepsilon_{\mathrm{R}}/\hbar\nu_s)^2/2$ and $\sqrt{1-T_l} \approx 1 - T_l/2$ we then find from Eq. (4):

$$T_{2b,R,s}^{\mathrm{P(AP)}} = \frac{T_{1,s}T_{2,s}}{\left(T_{1,s}+T_{2,s}\right)^2/4 + (\varepsilon_{\mathrm{R}}/\hbar\nu_s)^2} = \frac{\Gamma_{1,s}\Gamma_{2,s}}{(\Gamma_s/2)^2 + (\varepsilon_{\mathrm{R}}/\hbar)^2}\,, \tag{13}$$

where $\Gamma_{l,s} = \nu_s T_{l,s}$ are the tunnel rates for an electron approaching the barriers from FM^t, FM^w regions with energy E, respectively and $\Gamma_s = \Gamma_{1,s} + \Gamma_{2,s}$. Eq. (13), with its characteristic lorentzian lineshape, is known as the Breit-Wigner formula [7]. However the deviations from the exact result (4) can be quite large if the barriers transparencies approach unity. With large applied voltages, the width (at half-height, see Fig. 5) of the peaks becomes larger.

The maximum values of transmission coefficients versus the applied voltage are shown in Fig. 6, which are calculated from formula (10). Denotes of lines are the same as in Fig. 3. It can be seen that for some values of the applied voltage V, the transmission coefficients for some

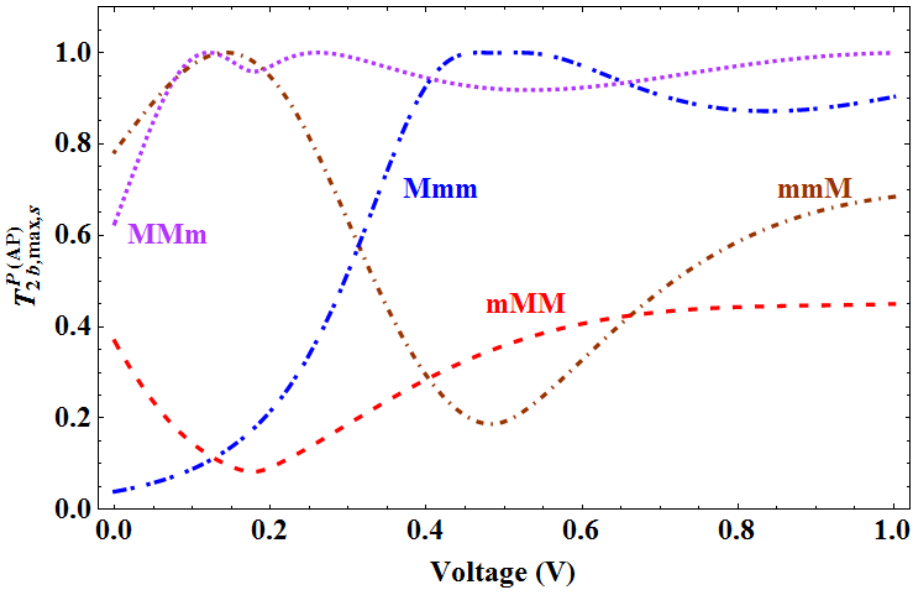

Figure 6. Dependences of the maximum value of the transmission coefficient vs applied bias across the asymmetrical DAMTJ for four spin conduction channels (as denoted by previous figures).

spin conduction channels can be equal to one. The transmission coefficient peaks (about unit) appear at voltage 0.125, 0.15, 0.27, 0.45, 0.55 and 1.0 V in the interval $0 \leq V \leq 1.0$, for different spin conduction channels.

4. Spin-polarized conductance and tunnel magnetoresistance

If the voltage is applied to the DAMTJ the spin-polarized conductance is generated. This conductance is induced by the quantum tunneling through the barriers. It is very small and decays exponentially with an increase in the thickness of the insulators. However, the FM^w layer is represents a quantum well. The motion of electrons in the FM^w layer is quantized. For some parameters of the structure $FM^t/I_1/FM^w/I_2/FM^b$ there arise resonant conditions. Then the spin-polarized tunneling conductance will rapidly increase at specific values of the applied voltage. Note that we already performed the calculation of spin-polarized tunnel conductance for planar symmetric and asymmetric DBMTJ [14, 20]. In this work, the spin-polarized tunnel conductance through the asymmetrical DAMTJ with the cross-sectional area of the radius a is calculated by the formula

$$G_s^{\mathrm{P(AP)}} = G_0 \frac{\left(k_{\mathrm{F},s}^{t(b)} a\right)^2}{2} \left\langle \cos\theta_{t(b),s} T_{2b,s}^{\mathrm{P(AP)}} \left(V, \cos\theta_{t(b),s}\right) \right\rangle, \tag{14}$$

where G_0 is the conductance quantum ($G_0 = 3.87 \times 10^{-5}\,\mathrm{Ohm}^{-1}$). The index t or b is selected by depending on polarity of the applied voltage V. The angle brackets denote averaging over the angles φ and $\theta_{t(b),s}$. The angle φ lies in the contact plane. The polar angle $\theta_{t(b),s}$ is defined by a trajectory of the motion of an electron in the top or bottom electrodes on the direction to the barrier. It is measured from the normal (see Fig. 1) to the contact plane. The absolute values of the Fermi wavevectors $k_{\mathrm{F},s}^{t(b)}$ correspond to the spin sub-bands of electrodes $FM^{t(b)}$. The index $s = \uparrow, \downarrow$ denotes the spin states of electrons in four spin conduction channels, see Fig. 2 and comments.

Note that strong dependence of the transmission coefficient on the position of quantum well states in the central FM^w layer lead to negative differential resistance. This is clearly seen in the dependences of the conductance on the applied voltage for different directions of magnetization of the FM^w layer. These dependences are not given in this paper. In Fig. 7, depen-

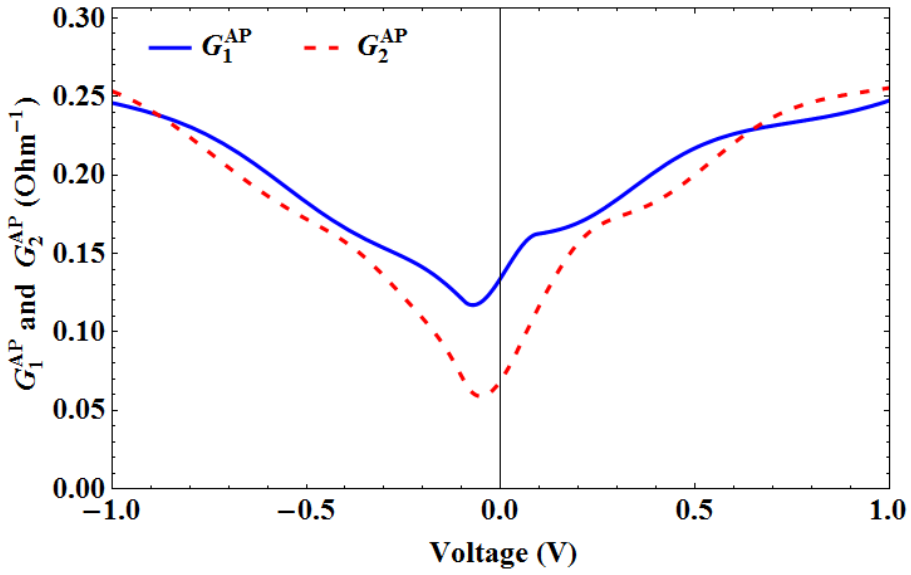

Figure 7. Dependencies of the tunnel conductances vs applied bias out of plane in the asymmetrical DAMTJ for two MMm+mmM (solid line) and Mmm+mMM (dashed line) of different channels at room temperature.

dences of the tunnel conductance vs applied bias in the $G_1^{\rm AP} = G_{\uparrow}^{\rm MMm} + G_{\downarrow}^{\rm mmM}$ (solid line) and $G_2^{\rm AP} = G_{\uparrow}^{\rm Mmm} + G_{\downarrow}^{\rm mMM}$ (dashed line) are the sums of the spin-up and spin-down conductance for at AP alignments of the magnetizations in the DAMTJ. The curves were calculated with the following parameters of the structure: the values of the Fermi wavevectors for electrons of the spin sub-bands of the FM layers are $k_{{\rm F},\uparrow}^{t} = 1.09\,{\rm Å}^{-1}$, $k_{{\rm F},\downarrow}^{t} = 0.68\,{\rm Å}^{-1}$, $k_{{\rm F},\uparrow}^{b} = 1.05\,{\rm Å}^{-1}$, $k_{{\rm F},\downarrow}^{b} = 0.71\,{\rm Å}^{-1}$, and $k_{{\rm F},\uparrow}^{w} = 1.01\,{\rm Å}^{-1}$, $k_{{\rm F},\downarrow}^{w} = 0.99\,{\rm Å}^{-1}$, respectively. The effective masses of conduction electrons in the ferromagnetic layers corresponded to the free electron mass m_e. The thicknesses of the dielectric oxide layers were taken $L_1 = 15.1$ Å, $L_2 = 19.1$ Å, and heights of the energy potentials above the Fermi energy are $U_1 = 0.24$ eV, $U_2 = 0.18$ eV. The effective masses of the electrons in the barriers were assumed to be $0.4m_e$. The thickness of the meddle FM^w layer was taken $L_w = 24.5$ Å.

The bias voltage dependence of the conductance is asymmetric with regard to positive and negative voltages when the magnetic electrodes are not identical and the barriers have different thicknesses. Also the prominent broad valleys in conductance at ∼0.15 V and ∼0.4 V, which are shown for $G_1^{\rm AP}$ and $G_2^{\rm AP}$ tunnel channels in DAMTJ, respectively. These may be ascribed to the consecutive coherent tunneling of certain spin conduction channel. The predominant elastic tunneling, where incident electrons from one electrode tunnel to the opposite electrode through the double-barrier without loss of energy, gives rise to a significant background to the conductance versus voltage curve.

Now, we consider the functional dependence of the TMR on the voltage drop across the DAMTJ and the change in its form as a function of the middle ferromagnetic layer FM^w and of the coercivity of the FM layers. It is known that the tunnel conductances of double barrier MTJs differ with different orientations of the magnetizations of adjacent FM layers and magnetic electrodes. Therefore, in our case of TMR, we have defined the relationship:

$$\mathrm{TMR} = \frac{G_1^{\rm AP} - G_2^{\rm AP}}{G_1^{\rm AP} + G_2^{\rm AP}} \cdot 100\%\,. \tag{15}$$

In Fig. 8, the TMR is shown as a function of the thickness L_w of the middle FM^w layer in the case of $V = 0.01$ V. The other parameters are the same as in Fig. 3. Some resonant features of the TMR curves are of particular interest: first, the TMR as a function of L_w shows well-defined

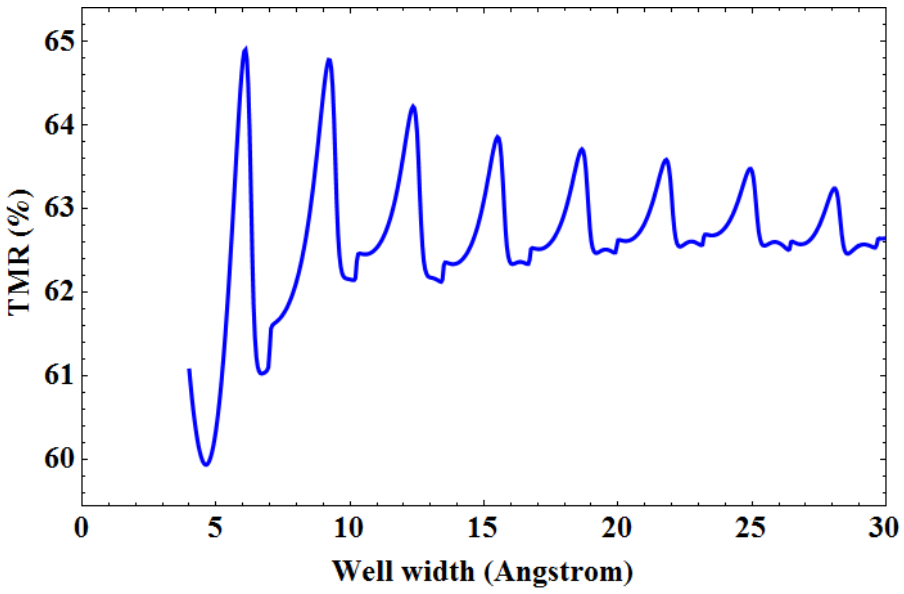

Figure 8. The tunnel magnetoresistance as a function of the middle ferromagnetic layer FM^w thickness L_w in the case of $V = 0.01$ V, calculated with the same parameters as in Fig. 3.

peaks, where the height of the peaks decreases monotonously with increasing L_w; secondly, the TMR peaks periodically repeat every 3.1 Å, corresponding to the wavevectors of the middle FM^w layer: $k^w_{\mathrm{F},\uparrow} = 1.1\,\text{Å}^{-1}$ and $k^w_{\mathrm{F},\downarrow} = 0.9\,\text{Å}^{-1}$, with $k^w_{\mathrm{F},\uparrow} = 0.8\,\text{Å}^{-1}$ and $k^w_{\mathrm{F},\downarrow} = 0.57\,\text{Å}^{-1}$ the period of oscillation of the TMR increases to 4.5 Å; thirdly, the TMR increases with increasing effective masses $m_{1(2)}$ of electrons in the insulating layers. This is not shown in Fig. 8. If the difference between the $k^w_{\mathrm{F},\uparrow}$ and $k^w_{\mathrm{F},\downarrow}$ wavevectors decreases, then the amplitude values of the TMR$\,(L_w)$ dependence decrease. If a non-magnetic metal is used instead of FM^w layer, for example, when $k^w_{\mathrm{F},\uparrow} = k^w_{\mathrm{F},\downarrow} = 0.57\,\text{Å}$, then TMR is zero.

Similar results for a DBMTJ structure with left and right ferromagnetic electrodes but with non-magnetic middle layer have been shown previously [12]. In this work the periodicity of the TMR magnitude was investigated for the first time, and it was found that TMR strongly correlates to quantum well states in the middle layer. The same finding is reproduced by our calculations. Thus, abrupt periodic variation of the TMR with increasing thickness L_w is related both to the quantum well states formed in the middle FM layer and to resonant tunneling through the whole structure.

In Fig. 9 dependences of tunnel magnetoresistance on the applied voltage V are show. The curves were calculated with the parameters are the same as in Fig. 3. The dashed curve is obtained at the maximum value of the transmission coefficient, see formula (10). Note that the change in thickness from 5 Å to 30 Å for the middle FM layer has almost no influence on the shape of the curve TMR, only the maximum value of the TMR changes. The effect of the voltage asymmetry at $V_{1/2}$ arises in the case of different initial set of wavevectors for the each layer. In addition, the asymmetry effect of the TMR curve is more pronounced under resonant conditions (dashed curve in Fig. 9).

The presented dependence of TMR (solid curve in Fig. 9) corresponds to the non-resonant electron tunneling through the DAMTJ. The theoretical calculations showed that the TMR values of FM/I/FM/I/FM heterostructures with top and bottom FM electrodes antiferromagnetically magnetized can reach up to 65%. The calculated TMR values are close to the experimental data [21, 22], which, however, were obtained for ordinary double-barrier MTJ.

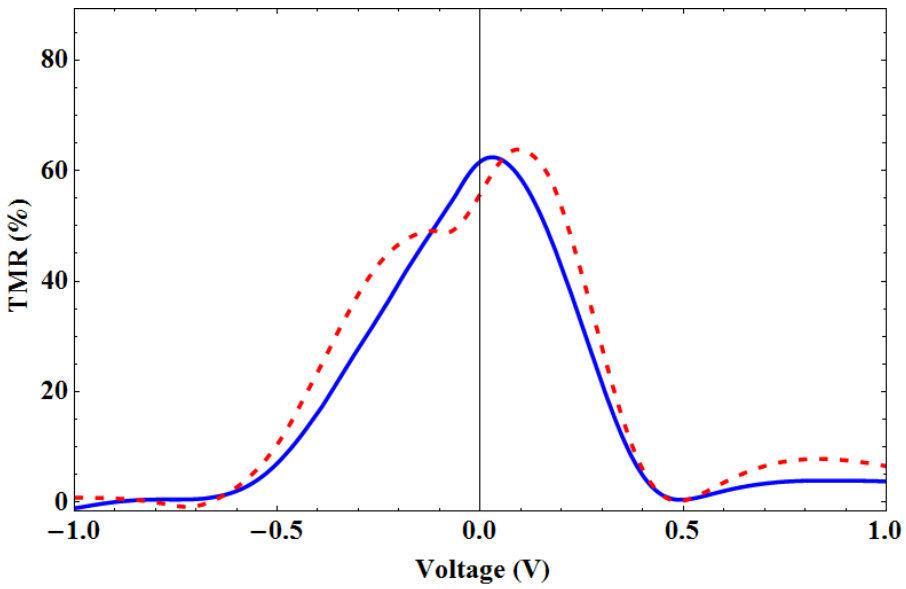

Figure 9. Bias dependence of TMR for L_w=25.0 Å. The dashed curve is obtained at the maximum value of the transmission coefficient, see formula (10). The other parameters at which the obtained TMR curves are the same as in Fig. 3.

5. Conclusion

Resonant tunneling has been studied theoretically in detail for the asymmetrical double-barrier antiferromagnetic structure with a ferromagnetic well under an applied voltage by taking into account the mass difference between the FM layers and the barrier layers. The analytical expressions of the transmission coefficients and resonance conditions, Eqs. (4), (9), and (10), have been derived by the transfer matrix method using the Airy function and taking into account the spin degrees of freedom. The transmission coefficient versus the phase difference has been examined and was shown that it has the characteristic lorentzian Breit-Wigner lineshape. It is confirmed that the unity resonance occurs if both conditions, (9) and $T_{1,s} = T_{2,s} = T_s$, are satisfied simultaneously, while the under-unity resonance occurs if only the condition $T_{1,s} = T_{2,s} = T_s$ is satisfied. Strong dependence of the transmission coefficient on the position of quantum well states in the middle layer lead to negative differential resistance. It is believed that the derived two conditions, (9) and $T_{1,s} = T_{2,s} = T_s$, and the above results could be useful for obtaining resonance energies and for fabricating resonant magnetic tunneling devices.

We have calculated tunnel magnetoresistance in the ballistic tunneling regime in a double-barrier antiferromagnetic junction with a magnetic central electrode. We showed that in some cases the resonant tunneling can give rise to large TMR. The calculations were performed under several approximations. First, we assumed that electron spin is conserved in tunneling events. It is, however, well known that TMR is reduced when spin-flip tunneling processes are allowed, despite the fact that such processes usually increase electric current by opening new channels for electron tunneling. Other scattering processes leading to incoherent tunneling can reduce the TMR value as well. Second, we used a simple free-electron-like model to describe electronic structure of the junction. In real ferromagnetic heterojunction however, electronic structure is much more complex, which can lead to quantitative modifications of the results presented here. Nevertheless some qualitative features of TMR will survive. The large TMR value we obtained in our numerical calculations followed from a specific position of the electron spin subbands in the ferromagnetic electrodes. Another approximation used in our description is the room temperature. We considered this case since the physical picture is then clear and one can easily explain all the features of the resonances and TMR. Generally, one may expect an increase in the tunneling conductance with increasing temperature and a decrease in TMR. It is shown that the TMR crucially depends on the middle layer thickness and the conduction band spin-polarizations in FM layers, by cause of the spin-polarized resonant states in the middle ferromagnetic layer. This illustrates the fact that some regimes of operation of the DAMTJ can be used for the effect of spin filtering of currents. The theory can be used for explanation of the tunneling characteristics with the diode effect, and searching for condition of softening the requirements to magnitude of the current necessary for switching the tunnel magnetic structures between high and low resistive states.

Acknowledgments

The work is partially funded by the Program of Competitive Growth of Kazan Federal University and partially supported by RFBR, research project no. 18-02-00204.

References

1. Kronmüller H., Parkin S. (eds.) *Handbook of Magnetism and Advanced Magnetic Materials*, Vol. 5: *Spintronics and Magnetoelectronics*, John Wiley & Sons (2007)
2. Xu Y., Awschalom D.D., Nitta J. (eds.) *Handbook of Spintronics*, Springer Science + Business Media Dordrecht (2016)

3. Tao B.S., Yang H.X., Zuo Y.L., Devaux X., Lengaigne G., Hehn M., Lacour D., Andrieu S., Chshiev M., Hauet T., Montaigne F., Mangin S., Han X.F., Lu Y. *Phys. Rev. Lett.* **115**, 157204 (2015)
4. Yang H., Yang S.-H., Parkin S.S.P. *Nano Letters* **8**, 340 (2008)
5. Sheng L., Chen Y., Teng H.Y., Ting C.S. *Phys. Rev. B* **59**, 480 (1999)
6. Wang Y., Lu Z.-Y., Zhang X.-G., Han X.F. *Phys. Rev. Lett.* **97**, 087210 (2006)
7. Breit G., Wigner E. *Phys. Rev.* **49**, 519 (1936)
8. Tsu R., Esaki L. *Appl. Phys. Lett.* **22**, 562 (1973)
9. Chang L.L., Esaki L., Tsu R. *Appl. Phys. Lett.* **24**, 593 (1974)
10. Martinek J., Barnaś J., Fert A., Maekawa S., Schön G. *J. Appl. Phys.* **93**, 8265 (2003)
11. Miyamoto K., Yamamoto H. *J. Appl. Phys.* **84**, 311 (1998)
12. Wilczynski M., Barnas J. *JMMM* **221**, 373 (2000)
13. Tagirov L.R., Vodopyanov B.P., Efetov K.B. *Phys. Rev. B* **63**, 104428 (2001)
14. Useinov N.Kh. *Phys. Solid State* **55**, 659 (2013)
15. Landau L.D., Lifshitz E.M. *Quantum Mechanics: Non-Relativistic Theory*, 3rd ed., Elsevier Butterworth-Heinemann (2005)
16. Burstein E., Lundqvist S. (eds.) *Tunneling Phenomena in Solids*, Plenum, New York (1969)
17. Mazierska J., Ledenyov D., Jacob M., Krupka J. *Supercond. Sci. Technol.* **18**, 18 (2005)
18. Faure-Vincent J., Tiusan C., Bellouard C., Popova E., Hehn M., Montaigne F., Schuhl A. *Phys. Rev. Lett.* **89**, 107206 (2002)
19. Buttiker M. *IBM J. Res. Dev.* **32**, 63 (1988)
20. Useinov N.Kh., Petukhov D.A., Tagirov L.R. *JMMM* **373**, 27 (2015)
21. Colis S., Gieres G., Bär L., Wecker J. *Appl. Phys. Lett.* **83**, 948 (2003)
22. Zeng Z.M., Wang Y., Han X.F., Zhan W.S., Zhang Z. *Eur. Phys. J. B* **52**, 205 (2006)